SPANDIDOS PUBLICATIONS

ONCOLOGY LETTERS 15: 5517-5532, 2018

MicroRNA-124-3p expression and its prospective functional pathways in hepatocellular carcinoma: A quantitative polymerase chain reaction, gene expression omnibus and bioinformatics study

RONG-QUAN HE[1*], XIA YANG[2*], LIANG LIANG[3], GANG CHEN[2*] and JIE MA[1*]

Departments of [1]Medical Oncology, [2]Pathology and [3]General Surgery, First Affiliated Hospital of Guangxi Medical University, Nanning, Guangxi Zhuang Autonomous Region 530021, P.R. China

Received January 18, 2017; Accepted December 14, 2017

DOI: 10.3892/ol.2018.8045

Abstract. The present study aimed to explore the potential clinical significance of microRNA (miR)-124-3p expression in the hepatocarcinogenesis and development of hepatocellular carcinoma (HCC), as well as the potential target genes of functional HCC pathways. Reverse transcription-quantitative polymerase chain reaction was performed to evaluate the expression of miR-124-3p in 101 HCC and adjacent non-cancerous tissue samples. Additionally, the association between miR-124-3p expression and clinical parameters was also analyzed. Differentially expressed genes identified following miR-124-3p transfection, the prospective target genes predicted *in silico* and the key genes of HCC obtained from Natural Language Processing (NLP) were integrated to obtain potential target genes of miR-124-3p in HCC. Relevant signaling pathways were assessed with protein-protein interaction (PPI) networks, Gene Ontology (GO) enrichment analysis, Kyoto Encyclopedia of Genes and Genomes (KEGG) and Protein Annotation Through Evolutionary Relationships (PANTHER) pathway enrichment analysis. miR-124-3p expression was significantly reduced in HCC tissues compared with expression in adjacent non-cancerous liver tissues. In HCC, miR-124-3p was demonstrated to be associated with clinical stage. The mean survival time of the low miR-124-3p expression group was reduced compared with that of the high expression group. A total of 132 genes overlapped from differentially expressed genes, miR-124-3p predicted target genes and NLP identified genes. PPI network construction revealed a total of 109 nodes and 386 edges, and 20 key genes were identified. The major enriched terms of three GO categories included regulation of cell proliferation, positive regulation of cellular biosynthetic processes, cell leading edge, cytosol and cell projection, protein kinase activity, transcription activator activity and enzyme binding. KEGG analysis revealed pancreatic cancer, prostate cancer and non-small cell lung cancer as the top three terms. Angiogenesis, the endothelial growth factor receptor signaling pathway and the fibroblast growth factor signaling pathway were identified as the most significant terms in the PANTHER pathway analysis. The present study confirmed that miR-124-3p acts as a tumor suppressor in HCC. miR-124-3p may target multiple genes, exerting its effect spatiotemporally, or in combination with a diverse range of processes in HCC. Functional characterization of miR-124-3p targets will offer novel insight into the molecular changes that occur in HCC progression.

Correspondence to: Professor Gang Chen, Department of Pathology, First Affiliated Hospital of Guangxi Medical University, 6 Shuangyong Road, Nanning, Guangxi Zhuang Autonomous Region 530021, P.R. China
E-mail: chen_gang_triones@163.com

Professor Jie Ma, Department of Medical Oncology, First Affiliated Hospital of Guangxi Medical University, 6 Shuangyong Road, Nanning, Guangxi Zhuang Autonomous Region 530021, P.R. China
E-mail: majie086@163.com

*Contributed equally

Key words: hepatocellular carcinoma, microRNA-124-3p, reverse transcription-quantitative polymerase chain reaction, gene expression omnibus, natural language processing, functional analysis

Introduction

MicroRNAs (miRNAs/miRs) are a class of short endogenous non-coding RNAs that suppress gene expression by either degrading mRNA or repressing mRNA translation through complementary binding to their specific target mRNAs in the 3'-untranslated region (1,2). Mature miRNAs are small single-stranded RNAs 19-22 nucleotides in length. Increasing evidence suggests that miRNAs are involved in diverse basic biological processes, including cell proliferation, apoptosis and differentiation (3,4). Studies have also verified that miRNAs are ectopically expressed in tumors and operate as tumor oncogenes or suppressors during tumor progression, indicating the potential for miRNAs as biomarkers for cancer diagnosis and therapy (2).

Hepatocellular carcinoma (HCC) is the third leading cause of global cancer-associated mortality, with the highest incidence occurring in Asia (5). The World Health Organization (WHO) estimates that there are ~56,400 newly diagnosed cases of HCC worldwide per year (6), with a significantly

higher occurrence in males. Notably, more than half of all HCC cases are diagnosed in China (7). Multiple risk factors contribute to the occurrence of HCC, including chronic viral hepatitis and alcohol abuse. HCC development typically involves several steps, progressing from chronic hepatitis, cirrhosis and dysplastic nodules to HCC (8). It has been revealed that miRNAs serve a pivotal role in HCC progression and may provide novel insight for diagnostic and therapeutic HCC strategies (9). miR-124-3p has been implicated in HCC and its expression has been demonstrated to be downregulated in HCC tissues (2,10). Additionally, several target genes of miR-124-3p have been discovered (2,10,11). However, to the best of our knowledge, previous studies combining gene expression omnibus (GEO) data and bioinformatics analysis to explore the mechanisms underlying the role of miR-124-3p in HCC have not been performed. Additionally, previous studies have only focused on a specific target gene of miR-124-3p. Therefore, the potential mechanisms by which miR-124 suppresses tumorigenesis in HCC remain unclear; miR-124-3p may be involved in the regulation of several other undiscovered mRNAs and signaling pathways. The present study investigated miR-124-3p expression and its potential target genes in HCC by combining reverse transcription-quantitative polymerase chain reaction (RT-qPCR) with GEO data, using prediction software and natural language processing (NLP).

The clinical significance of miR-124-3p expression in hepatocarcinogenesis and development and the potential target genes of functional pathways in HCC patients was analyzed. Gene expression profiles were examined from primary HCC samples, literature searches using PubMed were performed and microarray data was downloaded from GEO. miR-124-3p was transfected into the HepG2 cell line to confirm the prospective targeted genes predicted *in silico* (relevant data were downloaded from GSE6207, GEO Profiles) and key genes of HCC were identified from NLP. The identified differentially expressed genes (DEGs) were subsequently integrated to confirm the potential target genes of miR-124-3p in HCC. Finally, the relevant signaling pathways in HCC were assessed to determine the key genes involved in the maintenance of these pathways, in order to further identify novel therapeutic targets in HCC.

Materials and methods

Tissue specimens. A total of 101 formalin-fixed, paraffin-embedded (FFPE) HCC tissues (80 males and 21 females) with clear pathology diagnoses were collected (10% neutral formalin-fixed for 24 h at room temperature). These HCC patients underwent primary surgical resection at the First Affiliated Hospital of Guangxi Medical University (Nanning, China) between January 2012 and February 2014 and did not receive any additional treatment. The age of the HCC patients ranged from 29 to 82 years old, with a mean age of 52 years. Among the 101 cases, 70 were successfully followed up. Clinical stages were classified according to the WHO Tumor-Node-Metastasis (TNM) criteria (12). Recurrence-free survival (RFS) was defined as the length of time between surgery and recurrence. Additionally, 101 adjacent non-HCC tissues were obtained to serve as internal controls. The present study was approved by the Research Ethics Committee of the First Affiliated Hospital of Guangxi Medical University (Nanning, China), and written informed consent was obtained from all patients.

RNA extraction and RT-qPCR. The total RNA, including miRNA, was isolated from tumor sections using the miRNeasy FFPE kit (Qiagen China Co., Ltd., Shanghai, China), as previously described (13-15). The miScript Reverse Transcription and the miScript SYBR-Green PCR kits (218073 and 218161 respectively; Qiagen China Co., Ltd.) were used to evaluate miR-124-3p expression levels. Reverse transcription-quantitative polymerase chain reaction (RT-qPCR) was performed in triplicate using the 7900HT PCR system (Applied Biosystems; Thermo Fisher Scientific, Inc., Waltham, MA, USA), in order to determine miRNA expression. The following temperature protocol was applied: 16˚C for 30 min, 42˚C for 30 min and 85˚C for 5 min. LightCycler 480 SYBR-Green I Master (Roche Diagnostics GmbH) was used for qPCR, with the following thermocycling conditions: Initial pre-denaturation for 5 min at 95˚C, followed by 40 cycles of 95˚C with 10 sec, 60˚C for 10 sec and 72˚C for 10 sec; evaluation of the solubility curve was performed at 95˚C for 5 sec and 65˚C for 1 min, which was followed by cooling at 40˚C for 30 sec. Each experiment was repeated in triplicate. The abundance of miR-124-3p in each sample was normalized to references genes RNU6B and RNU48, which was demonstrated to be a stable internal control in previous studies (16). The sequences purchased from Applied Biosystems (Thermo Fisher Scientific, Inc.) were as follows: miR-124-3p, 5'-UCGGGGAUCAUCAUGUCACGAG-3' (cat. no. 4427975-001288), RNU6B, 5'-CGCAAGGAUGACACG CAAAUUCGUGAAGCGUUCCAUAUUUUU-3' (cat. no. 4427975-001093); and RNU48, 5'-GAUGACCCCAGGUAA CUCUGAGUGUGUCGCUGAUGCCAUCACCGCAGCGCU CUGACC-3' (cat. no. 4427975-001006). The relevant expression of miR-124-3p was quantified using the formula $2^{-\Delta Cq}$ (17).

Literature review search. PubMed was searched to identify previous studies regarding miR-124-3p expression, and clinical parameters were also collected if available. The search terms were as follows: 'malignant* OR cancer OR tumor OR neoplas* OR carcinoma', 'hepatocellular OR liver OR hepatic OR HCC' and 'miR-124 OR miRNA-124 OR microRNA-124 OR 'miR 124' OR 'miRNA 124' OR 'microRNA 124' OR miR-124-3p OR miRNA-124-3p OR microRNA-124-3p'. A meta-analysis with P-values alone was subsequently conducted to pool the collected data if no relative expression of miR-124-3p was provided. To allow the combination of the P-values from each study, two-tailed P-values were converted into one-tailed P-values by dividing by two. A meta-analysis using Fisher's method was subsequently performed (18).

Public microarray data analysis of miR-124-3p. To verify the difference in miR-124-3p expression between HCC and normal liver tissues, the GEO database of the National Center for Biotechnology Information (NCBI) of the National Institute of Health (NIH; http://www.ncbi.nlm.nih.gov/geo/) and the ArrayExpress data of the European Bioinformatics Institute (EBI; http://www.ebi.ac.uk/arrayexpress/) were searched. The following terms were searched: 'malignant* OR cancer OR tumor OR neoplas* OR carcinoma',

'hepatocellular OR liver OR hepatic OR HCC' and 'miR-124 OR miRNA-124 OR microRNA-124 OR 'miR 124' OR 'miRNA 124' OR 'microRNA 124' OR miR-124-3p OR miRNA-124-3p OR microRNA-124-3p'. Following screening, seven datasets [GSE57555 (https://www.ncbi.nlm.nih.gov/geo/query/acc.cgi?acc=GSE57555) (19), GSE41874 (https://www.ncbi.nlm.nih.gov/geo/query/acc.cgi?acc=GSE41874), GSE40744 (https://www.ncbi.nlm.nih.gov/geo/query/acc.cgi?acc=GSE40744) (20), GSE21362 (https://www.ncbi.nlm.nih.gov/geo/query/acc.cgi?acc=GSE21362) (21), GSE20077 (https://www.ncbi.nlm.nih.gov/geo/query/acc.cgi?acc=GSE20077) (22), GSE12717 (https://www.ncbi.nlm.nih.gov/geo/query/acc.cgi?acc=GSE12717) (23) and GSE31383 (https://www.ncbi.nlm.nih.gov/geo/query/acc.cgi?acc=GSE31383) (24)] were included. Among them, dataset GSE57555 contained 11 cholangiocarcinoma samples, 5 HCC samples and 16 normal controls; GSE41874 contained 3 primary HCC samples, 3 metastatic hepatocellular carcinoma (metastatic HCC) samples and 4 normal controls; GSE40744 contained 9 HCC, 17 HCC surrounding non-tumorous tissue affected by cirrhosis (HCC-CIR), 18 hepatitis C virus-associated cirrhosis without HCC (CIR), 13 hepatitis B virus-associated acute liver failure (ALF), 7 surrounding normal liver of liver angioma (NLA) and 12 non-cancerous liver tissues; GSE21362 contained 73 HCC and 73 normal control samples; GSE20077 was a cell line dataset, which contained 7 HCC cell lines and 3 normal primary human hepatocytes; GSE12717 contained 10 HCC and 6 normal control samples; GSE31383 contained 9 HCC and 10 normal control samples. In addition, a dataset GSE64989 contained 8 recurrent HCC and 10 non-recurrent HCC samples, and two datasets [GSE67138 (https://www.ncbi.nlm.nih.gov/geo/query/acc.cgi?acc=GSE67138) and GSE67139 (https://www.ncbi.nlm.nih.gov/geo/query/acc.cgi?acc=GSE67139)] about vascular invasion were also included. GSE67138 contained 23 vascular invasion and 34 non-vascular invasions; GSE67139 contained 58 vascular invasion and 57 non-vascular invasions. The significant differences between the case groups and normal controls for the included datasets were calculated using Student's t-test.

To explore the DEGs associated with miR-124-3p in HCC, GEO profiles were searched with the terms 'HCC AND miR-124-3p' and a gene set (GSE6207) investigated miR-124-3p transfection in the HepG2 cell line was identified. The effects in the miR-124 overexpression group with the negative control group were subsequently compared by assessing fold change (FC), to identify downregulated genes and potential miR-124 targets (FC <0.95 were selected). The GSE6207 dataset (25) was retrieved to explore the mechanism by which miR-124-3p may be involved in hepatocarcinogenesis.

In silico analysis of target genes of miR-124-3p. Predicted targets of miR-124-3p and its target sites were analyzed using miRWalk2.0 (http://zmf.umm.uni-heidelberg.de/apps/zmf/mirwalk2/) (26), which combines 12 existing miRNA-target prediction programs (miRWalk, Microt4, miRanda, miRbridge, miRDB, miRMap, miRNAMap, Pictar2, PITA, RNA22, RNAhybrid and TargetScan) to provide comprehensive potential targets for miR-124-3p. The genes contained in >5 prediction software programs were selected in order to obtain more reliable targets.

NLP. NLP is a novel computerized approach to analyze text in order to achieve human-like language processing. Under this approach, programmers create software to 'read' the text and extract key pieces of information from clinical notes, procedures, radiology or pathology reports and laboratory results (27,28). A literature search was performed in PubMed to obtain all associated electronic records. The literature search queries were as follows: (hepatocellular carcinoma) AND (resistance OR prognosis OR metastasis OR recurrence OR survival OR carcinogenesis OR sorafenib OR bevacizumab) and ['1980/01/01' (PDAT): '2015/05/25' (PDAT)]. Subsequently, all pertinent molecules were retrieved and a list was generated, primarily comprising proteins and genes. Gene mention tagging was conducted with A Biomedical Named Entity Recognizer (ABNER; http://pages.cs.wisc.edu/~bsettles/abner/). ABNER also assisted in conjunction resolution. Gene name normalization conformed to the standard names in the Entrez database provided by NCBI (https://www.ncbi.nlm.nih.gov/gene/). Finally, statistical analysis was performed; P<0.01 was considered to indicate a statistically significant difference, as previously described (29,30). The P-value of a certain HCC-related gene was calculated with the following formula:

$$P = 1 - \sum_{i=0}^{k-1} p(i \mid n, m, N);$$

$$p(i \mid n, m, N) = \frac{n!(N-n)!m!(N-m)!}{n-i!i!n-m!N-n-m+i!N!}$$

Where N indicates all the eligible studies, m is the frequency of the related genes, n is the frequency of HCC and k is the co-occurrence of HCC and a certain gene.

Construction of protein-protein interaction (PPI) networks. Overlapping genes were placed into the Search Tool for the Retrieval of Interacting Genes/Proteins (STRING; version 10.0; http://string-db.org/) to construct the PPI network. The direct (physical) and indirect (functional) associations between the proteins were identified using four methods: Literature-reported protein interactions, high-throughput experiments, genome analysis and prediction, and co-expression studies. A node with a degree of high connectivity was perceived as a hub node. By scrutinizing the connectivity degrees of the nodes in the PPI networks, the hub genes were determined. Subsequently, the expression of hub genes identified from PPI networks were calculated with TCGA data. Firstly, the publicly available RNA-seq data of the mRNA level of Liver hepatocellular carcinoma (LIHC) samples were downloaded directly from the TCGA data portal (https://tcga-data.nci.nih.gov/tcga/tcgaHome2.jsp) via bulk download mode [LIHC (cancer type), RNASeqV2 (data type), level 3 (data level)]. Then the relative expression of these hub genes were extracted and calculated on a log2 scale to investigate the potential targets of miR-124-3p in HCC. The immunohistochemical data of most potential targets of miR-124-3p were downloaded from The Human Protein Atlas (http://www.proteinatlas.org/).

Functional and signaling pathway analyses. Further functional and signaling pathway analyses were performed on a set of condition-specific genes, those that overlapped in the GEO database, target prediction software and NLP. The functional and signaling pathway analyses of the selected DEGs was performed on a public database platform; the Database for Annotation, Visualization and Integrated Discovery (DAVID; https://david.ncifcrf.gov/), which provides a functional interpretation of large lists of genes derived from genomic studies. The analyses also included Gene Ontology (GO) function analysis (http://www.geneontology.org/), Kyoto Encyclopedia of Genes and Genomes (KEGG) (http://www.genome.jp/kegg/) analysis and Protein Annotation Through Evolutionary Relationships (PANTHER) pathway analysis (http://www.pantherdb.org/). GO function analysis categorized the selected genes into groups, in accordance with the following three independent classification standards: Biological process (BP), cellular component (CC), and molecular function (MF). A Benjamini P-value of <0.05 was used to indicate a statistically significant difference in the above pathway enrichment analyses. The results were visualized as three GO maps using Cytoscape version 3.4.0 (http://cytoscape.org/). Subsequently, the pathway with the top priority was selected for further evaluation and the most significant aberrantly expressed genes were examined for their prospective diagnostic and prognostic value. The top 30 enriched pathways of KEGG were visualized using the ggplot2 (version 2.2.1) package of R/Bioconductor (version 3.4.2) Project for Statistical Computing (https://www.r-project.org).

Statistical analysis. SPSS 22.0 (IBM Corp., Armonk, NY, USA) was used for statistical analysis. All data are presented as the mean ± standard deviation. The receiver operating characteristic (ROC) curve was drawn to identify the diagnostic significance of miR-124-3p and clinical parameters. The criteria for assessing the area under the ROC curve (AUC) were as follows: 0.5-0.7, poor evidence for diagnosis; 0.7-0.9, moderate evidence for diagnosis; 0.9-1.0, high evidence for diagnosis. The correlations between miR-124-3p expression and clinicopathological parameters were determined using Spearman's rank correlation. Significant differences between HCC and non-cancerous liver tissues were analyzed using the Student's t-test. The significant differences amongst three groups was examined using one-way analysis of variance. Since no significant differences were identified, no post-hoc test was performed. A box-whisker plot was generated to demonstrate miR-124-3p expression from all GEO datasets using GraphPad Prism (version 5.0; GraphPad Software, Inc., La Jolla, CA, USA). RFS was assessed using the Kaplan-Meier method as well as Cox Regression and the log-rank test was performed to compare survival times. Kaplan-Meier survival curves were drawn to evaluate the association between miR-124-3p expression and the survival rate of 101 patients with HCC. P<0.05 was considered to indicate a statistically significant difference.

Results

Expression of miR-124-3p in HCC tissues and its association with clinical parameters. RT-qPCR analysis of miR-124-3p expression in 101 HCC and adjacent non-cancerous tissues revealed that the relative expression of miR-124-3p in HCC tissues was 2.4439±1.54599, which was significantly reduced compared with expression in the adjacent non-cancerous liver tissues (3.5279±1.82462; P<0.001). The AUC of the low miR-124-3p levels for HCC diagnosis was 0.691 (95% CI, 0.618-0.763; P<0.001; Fig. 1), with a cut-off value of 3.30, which indicated that miR-124-3p is a poor diagnostic marker for HCC. The expression of miR-124-3p in HCC samples with a single tumor node was significantly increased (2.7356±1.73799) compared with those with multiple tumor nodes (2.0659±1.16857; P=0.030). Compared with advanced stage HCC, the relative expression of miR-124-3p in early stage patients was markedly increased (stage I and II, 3.4600±1.97104; stage III and IV, 2.1096±1.21910; P=0.003). Spearman's rank correlation analysis revealed a correlation between miR-124-3p and clinical stage (r=-0.305; P=0.002). The clinicopathological parameters of the 101 HCC patients are presented in Table I.

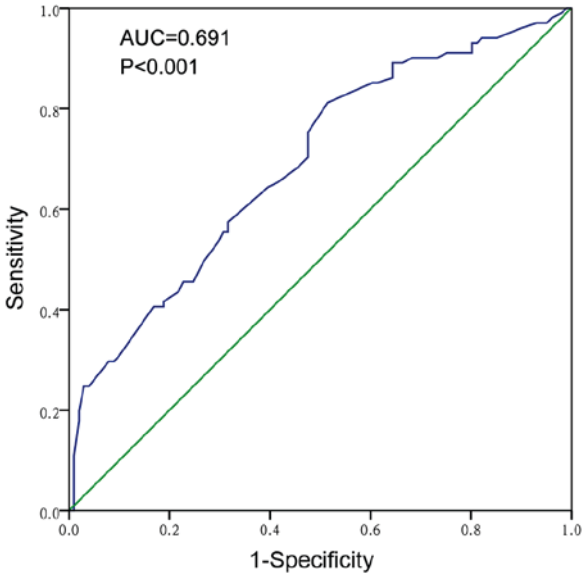

Figure 1. Receiver operating characteristic curve of the diagnostic value of miR-124-3p expression in HCC. The AUC of miR-124-3p was calculated to be 0.691 (95% CI, 0.618-0.763; P<0.001). AUC, area under curve; miR-124-3p, microRNA-124-3p.

Expression of miR-124-3p is correlated with the prognosis of patients with HCC. Kaplan-Meier analysis and Cox Regression were performed in order to determine the prognostic role of miR-124-3p. The follow-up information of 70 patients was obtained. In total, 44 patients exhibited low miR-124-3p expression (mean, <2.9859), while 26 patients exhibited high expression. The median survival time of the low miR-124-3p expression group was 57.00 months which was significantly reduced compared with that of the high expression group (the survival rate at each time point was >50%). The RFS rate was significantly reduced in the low miR-124-3p expression group compared with the high expression group (P=0.001; Fig. 2). The Cox Regression also demonstrated a hazard ratio of 0.069 (95%CI, 0.009-0.552; P=0.012).

Expression of miR-124-3p in eight GEO datasets and previous reports. To confirm the RT-qPCR results of the

Table I. Association between miR-124-3p and clinicopathological parameters in hepatocellular carcinoma.

		Relative miR-124-3p expression ($2^{-\Delta Cq}$)			Spearman's rank correlation	
Clinicopathological feature	n	Mean ± standard deviation	t	P-value	r	P-value
Tissue type						
Adjacent non-cancerous	101	3.5279±1.82462	-4.556	<0.001[a]	-	-
HCC	101	2.4439±1.54599				
Age, years						
≥50	51	2.2182±1.17362	-1.484	0.142	0.081	0.423
<50	50	2.6740±1.83446				
Sex						
Male	80	2.4642±1.62180	0.257	0.797	0.026	0.800
Female	21	2.3662±1.24620				
Differentiation						
High	7	1.6857±0.74482	0.985	0.377	0.038	0.704
Moderate	64	2.5442±1.60274				
Low	30	2.4067±1.54405				
Size						
<5 cm	21	2.4381±1.60171	-0.019	0.985	0.028	0.777
≥5 cm	80	2.4454±1.54141				
Tumor nodes						
Single	57	2.7356±1.73799	2.200	0.030[a]	-0.193	0.053
Multi	44	2.0659±1.16857				
Metastasis						
No	49	2.5980±1.85646	0.960	0.340	0.014	0.890
Yes	52	2.2987±1.18255				
Clinical TNM stage						
I-II	25	3.4600±1.97104	3.228	0.003[a]	-0.305	0.002[a]
III-IV	76	2.1096±1.21910				
Portal vein tumor embolus						
-	69	2.5571±1.62674	1.082	0.282	-0.082	0.414
+	32	2.1997±1.34728				
Vaso-invasion						
-	63	2.5705±1.66786	1.060	0.292	-0.070	0.485
+	38	2.2339±1.31371				
Tumor capsular infiltration						
With complete capsule	49	2.6039±1.71438	1.010	0.315	-0.060	0.552
No capsule or infiltration	52	2.2931±1.36838				
AFP						
-	46	2.3150±1.43969	0.314	0.755	-0.008	0.944
+	39	2.4205±1.66341				
Cirrhosis						
-	54	2.4148±1.33719	0.198	0.844	0.066	0.509
+	47	2.4772±1.77018				

t, Student's t-test; [a]P<0.05; miR-124-3p, microRNA-124-3p; TNM, tumor-node-metastasis; AFP, α-fetoprotein.

present study, GEO datasets were searched to compare the expression of miR-124-3p between HCC and non-cancerous tissues. miR-124-3p expression levels in all seven microarray chips [GSE57555 (19), GSE41874 (https://www.ncbi.nlm.nih.gov/geo/query/acc.cgi?acc=GSE41874), GSE40744 (20), GSE21362 (21) GSE20077 (22), GSE12717 (23) and

Table II. Identified potential target genes of microRNA-124-3p in hepatocellular carcinoma.

ZNF148	ZDHHC2	ZBTB20	YAP1	WSB1	WHSC1	WASF2	VIM	VASH1	UBE3C	TNFRSF10B	TLR7
TLN2	TJP1	TGFA	TFRC	TFPI	TET1	TCF4	TCF3	SULF1	ST8SIA2	SREBF1	SQSTM1
SPTBN1	SPRY2	SPRY1	SPHK1	SPARC	SPAG9	SP1	SOX9	SOS1	SORT1	SOD2	SMYD3
SMAD5	SMAD4	SEC62	SEC13	SART3	ROCK1	RELA	RAB27A	PVRL2	PTPN12	PTP4A1	PSEN1
PRRX1	PRLR	PPP1R13L	PPARA	PIK3CA	PEA15	PAQR3	NAAA	MYB	MTR	MTAP	MPZL1
MAPRE1	MAPK14	MAPK10	MAPK1	LRP6	LRP1	LOX	KLF4	KIF14	JAG1	ITGB1	IQGAP1
ING3	IL7R	IL11	IGFBP3	HTATIP2	HNMT	HLA-E	HIPK2	HDLBP	HDAC4	GYPA	GSN
GSC	GRIN1	GGPS1	G3BP1	FMNL2	FGFR2	FGFR1	ETS1	ERN1	ERBB3	ERBB2	EPHA7
EPHA3	EGR1	E2F5	DTL	DPP4	DLGAP5	DAB2IP	DAB2	CTGF	CRKL	CHEK1	CEACAM1
CDK6	CDK4	CDK2	CDC25B	CD44	CCNG2	CAPN2	C1GALT1	BMP6	BCL2L2	BCL2L11	AURKA
ASPH	ARHGDIA	ARHGAP1	ARAF	ANXA7	ANGPT2	AKT2	AHR	ABI1	ABCC4	ABCC12	ABCA2

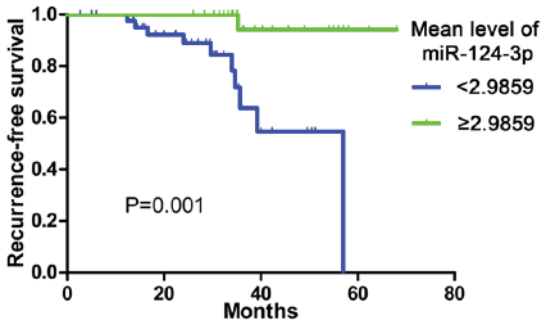

Figure 2. miR-124-3p expression and hepatocellular carcinoma survival. The Kaplan-Meier survival curve demonstrated that the median survival of the low miR-124-3p expression group was reduced compared with that of the high expression group. P=0.001. miR-124-3p, microRNA-124-3p; censored, patients lost to follow-up or succumbed to other causes (not HCC).

GSE31383 (24)], including 119 HCC and 124 non-cancerous tissues, were presented in Fig. 3. A recurrence [GSE64989 (31)] and two invasive datasets (GSE67139 and GSE67138) were also presented. Student's t-test revealed that miR-124-3p was significantly reduced in HCC compared to normal control samples with GSE 40744 data. While no significant difference could be found in other datasets. The seven datasets and RT-qPCR data from the present study were further analyzed by a meta-analysis, in which standardized mean differences (SMD) with a 95% CI [SMD and 95% CI, 0.01 (-0.38-0.40)] from selected datasets were pooled. However, no significant differences were observed between the HCC and non-cancerous liver groups (data not shown). Literatures review searching obtained four reliable studies. The PubMed literature search revealed that miR-124-3p expression in HCC was reduced compared with that in adjacent non-cancerous liver tissues, which was consistent with the results obtained in the present study (pooled P-value of four studies, $P=1.05x10^{-10}$).

Potential targets of miR-124-3p in HCC. To identify potential targets of miR-124-3p, GEO profiles were searched and gene chip data were downloaded such that the targets and functions of miR-124-3p could be analyzed. The fold-change (FC) between the miR-124 transfection group and the negative control group was subsequently calculated and FC values <0.95 were selected; a total of 4,261 mRNAs were attained following duplicate exclusion. The prediction process was then performed online using the miRWalk 2.0, which contained 12 computational algorithms. To increase the reliability of the present study, 3,902 mRNAs that appeared in ≥5 prediction software programs were screened, and any duplicates were excluded. Additionally, the titles and abstracts of 64,577 studies were included through the use of NLP data and text mining tools and a total of 1,800 HCC-associated genes were subsequently identified. The potential target mRNAs of miR-124-3p in HCC were determined by combining the predicted targets obtained using the three methods described earlier. In total, 132 mRNAs (Table II) were selected for PPI network analysis, GO analysis, KEGG pathway annotation and PANTHER pathway analysis, in order to identify the genes largely representative of the prospective molecular mechanism of miR-124-3p in HCC. A flow chart demonstrating the aforementioned process is presented in Fig. 4.

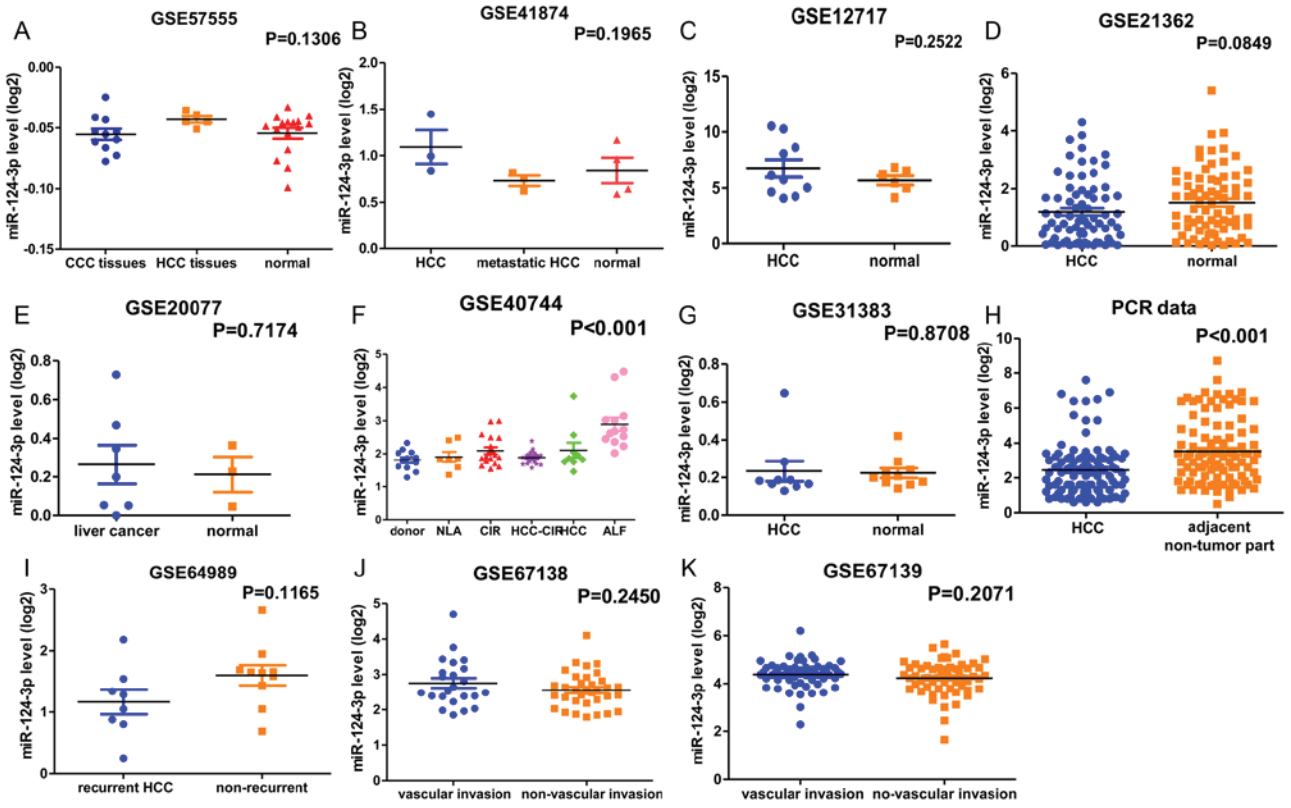

Figure 3. Scatter diagram presenting the miR-124-3p expression of 10 microarray chips. (A) miR-124-3p expression in CCC, HCC and adjacent non-cancerous tissues. P=0.1306. (B) miR-124-3p expression in primary HCC, metastatic HCC and normal tissues. P=0.1965. (C) miR-124-3p expression in HCC tissues and normal liver tissues. P=0.2522. (D) miR-124-3p expression in HCC tissues and non-cancerous tissues. P=0.0849. (E) miR-124-3p expression in a human liver cancer cell line and normal primary human hepatocytes. P=0.7174. (F) miR-124-3p expression in HCC, HCC-CIR, CIR, ALF, NLA and non-cancerous liver tissues. P<0.001. (G) miR-124-3p expression in HCC tissues and human healthy liver tissues. P=0.8708. (H) miR-124-3p expression in HCC and adjacent non-tumor tissues. P<0.001. (I) miR-124-3p expression in recurrent HCC tissues and non-recurrent HCC tissues. P=0.1165. (J) miR-124-3p expression in tumor vascular invasion tissues and non-tumor vascular invasion tissues. P=0.2450. (K) miR-124-3p expression in tumor vascular invasion tissues and non-tumor vascular invasion tissues. P=0.2071. miR-124-3p, microRNA-124-3p; HCC, hepatocellular carcinoma; CCC, cholangiocarcinoma; HCC-CIR, HCC surrounding non-tumorous tissue affected by cirrhosis; CIR, hepatitis C virus-associated cirrhosis without HCC; ALF, hepatitis B virus-associated acute liver failure; NLA, surrounding normal liver of liver angioma.

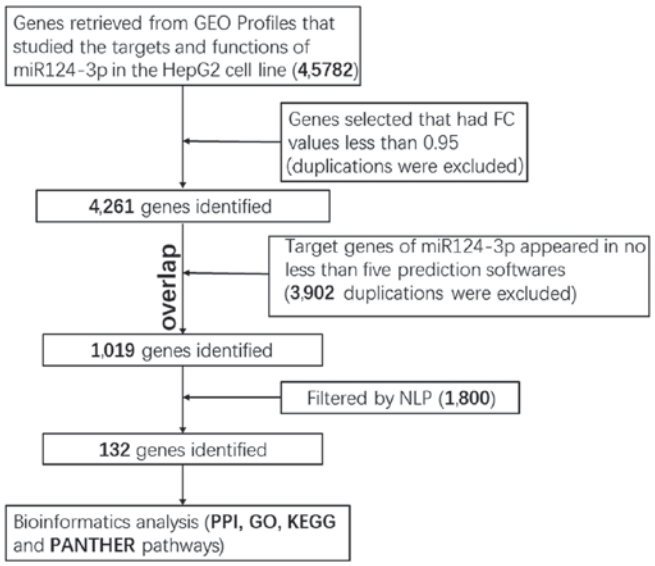

Figure 4. Illustration of the workflow pipeline. The genes selected for bioinformatics analysis overlapped in the GEO database, prediction software and NLP analysis, resulting in the identification of 132 genes. miR-124-3p, microRNA-124-3p; GEO, gene expression omnibus; FC, fold change; NLP, natural language processing; PPI, protein-protein interaction; GO, gene ontology; KEGG, Kyoto Encyclopedia of Genes and Genomes; PANTHER, Protein Annotation Through Evolutionary Relationships.

Analysis of PPI networks. The influence of multiple genes, interacting through a signaling pathway, on cellular function is more significant than the influence of a single gene. Therefore, a PPI network was constructed with 132 genes imported into the STRING software. Consequently, a total of 109 nodes and 386 edges were involved in the constructed network. Furthermore, 20 key genes with >10 nodes were identified, including mitogen-activated protein kinase 1 (MAPK1), MAPK14, early growth response 1 (EGR1), phosphatidylinositol-4,5-biphosphate 3-kinase catalytic subunit α (PIK3CA), RELA proto-oncogene, nuclear factor κ B subunit (RELA), SOS Ras/Rac guanine nucleotide exchange factor 1 (SOS1), SMAD family member 4 (SMAD4), erb-b2 tyrosine kinase 2, cyclin dependent kinase 2 (CDK2), ETS proto-oncogene 1, transcription factor (ETS1), Sp1 transcription factor (SP1), MYB proto-oncogene, transcription factor, fibroblast growth factor receptor 1 (FGFR1), AKT serine/threonine kinase 2 (AKT2), aurora kinase A, CDK4, FGFR2, SMAD5, MAPK10 and cell division cycle 25B. A total of 23 genes and proteins acted independently. PPI networks are presented in Fig. 5.

In order to further study the potential role of miR-124-3p and the 20 key genes identified in HCC, the literature was reviewed and validated prediction software was searched. The target genes that had been validated by a luciferase report assay were

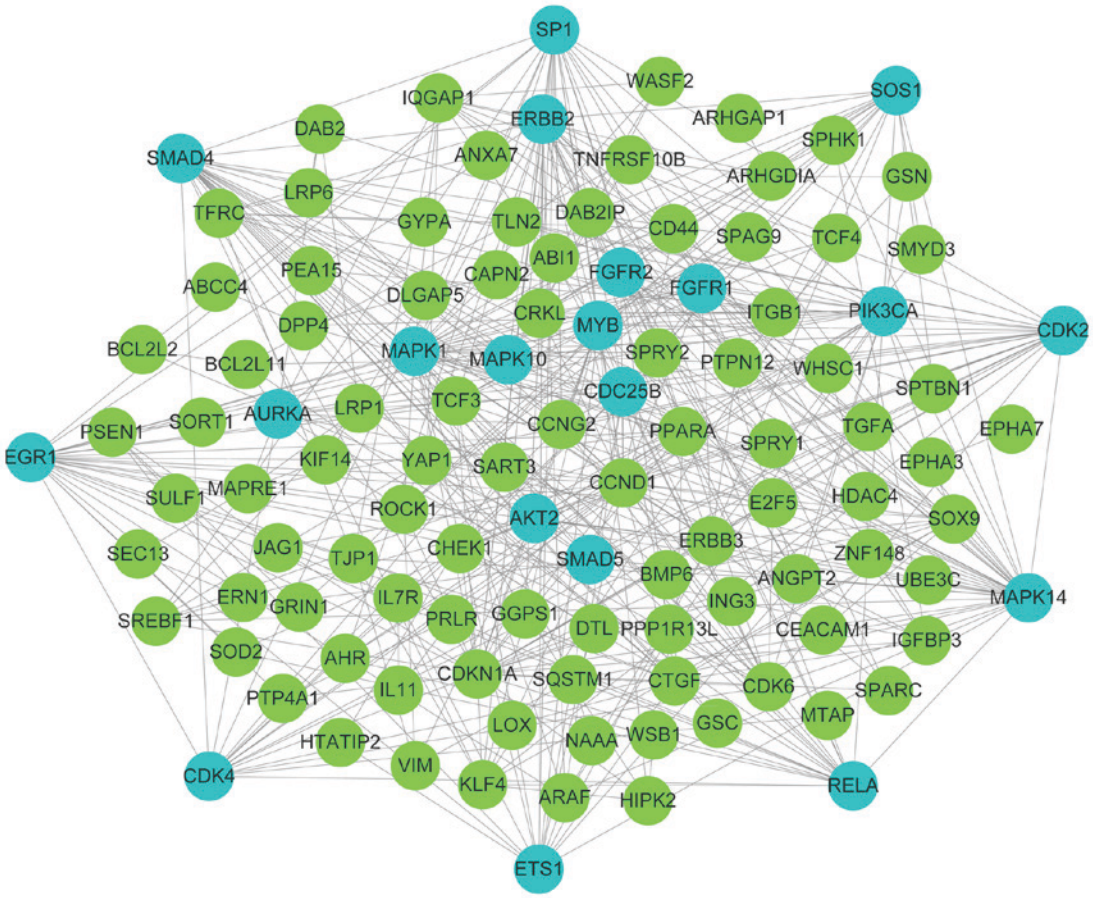

Figure 5. Protein-protein interaction network. Interactions among the prospective 132 target genes were illustrated using the Search Tool for the Retrieval of Interacting Genes/Proteins online database and Cytoscape v3.4.0. Network nodes represent proteins and edges represent protein-protein associations. The blue nodes indicate the identified key genes.

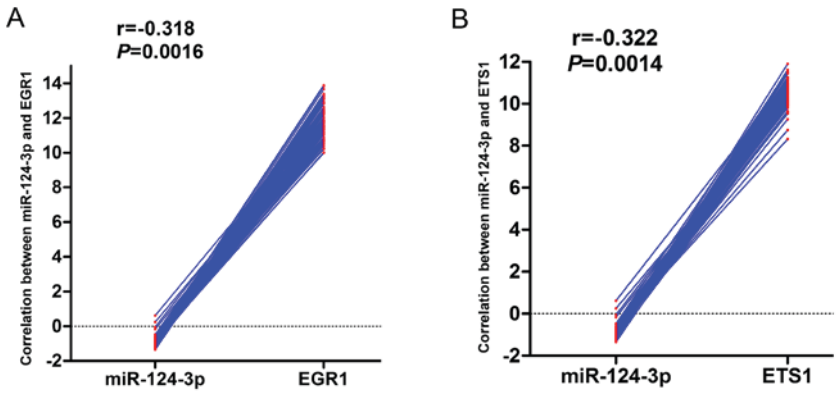

Figure 6. Correlation between microRNA 124-3p and (A) EGR1 or (B) ETS1 expression based on the GSE22058 dataset. EGR1, early growth response protein 1; ETS1, ETS proto-oncogene 1.

subsequently determined. The results revealed that MAPK14, EGR1, RELA, CDK2, CDK4, ETS1, SOS1 and SP1 were upregulated following miR-124-3p knockdown. GSE22058 data were also mined to examine the genome-wide expression profiles of miRNAs and mRNAs of 96 HCC samples and their adjacent non-cancerous liver tissues. This revealed that EGR1 and ETS1 were negatively correlated with miR-124-3p expression (Fig. 6). Additionally, validation of the association between miR-124-3p and the 20 identified key genes based on TCGA data was attempted, but insufficient data was available.

Validation of potential target gene expression based on TCGA with data from The Human Protein Atlas. Based on the literature review and prediction software search, 11/20 key genes identified by the PPI network were selected for further analysis, namely MAPK14, EGR1, RELA, PIK3CA, SOS1, SMAD4, CDK2, CDK4, ETS1, SP1 and AKT2. The relative expression of these 11 genes calculated with TCGA data revealed that no significant differences were detected in the expression of PIK3CA, SMAD4 and AKT2 between the HCC and adjacent non-cancerous liver tissues. EGR1 and ETS1 were

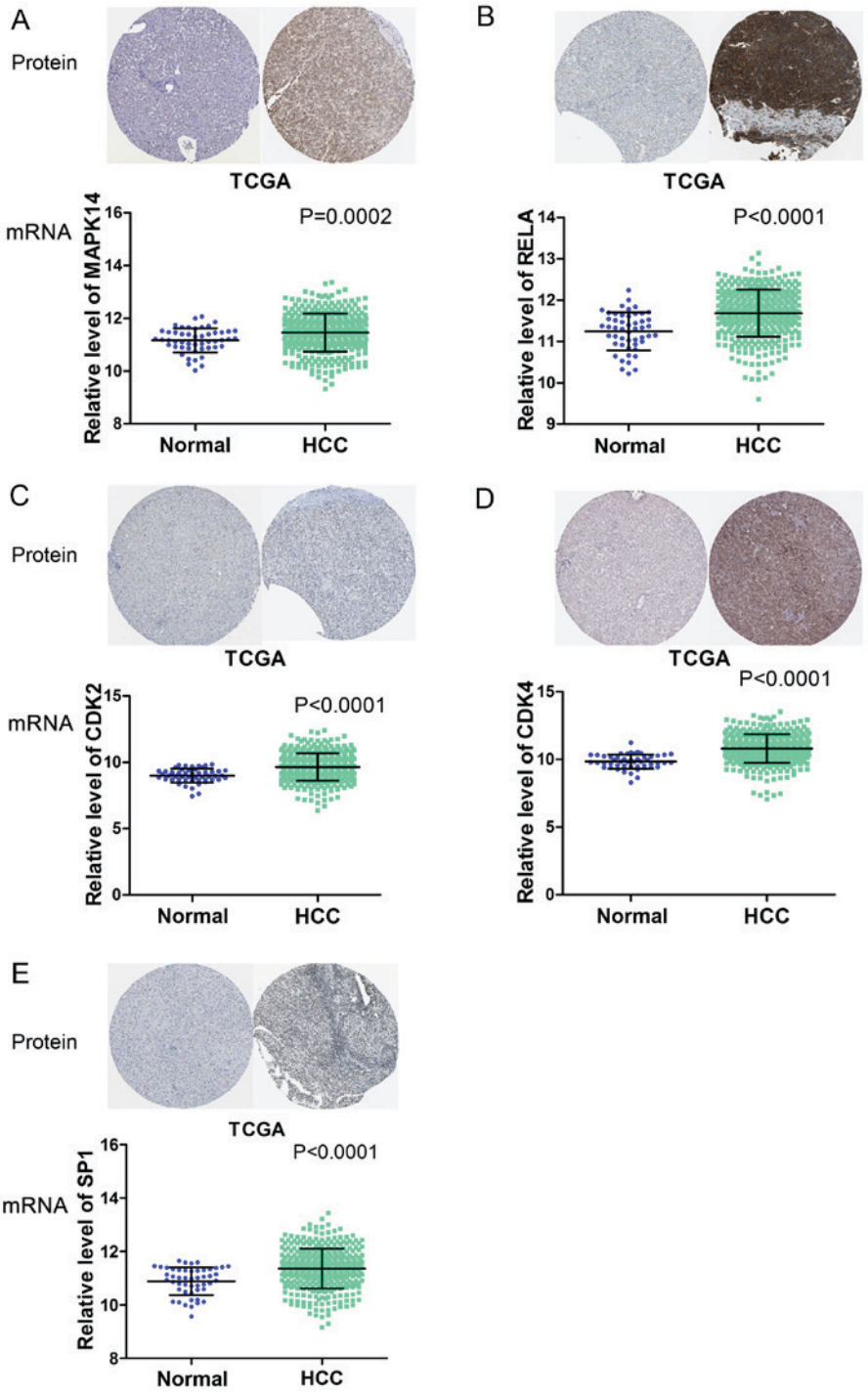

Figure 7. Overexpression of five potential target genes of microRNA 124-3p in HCC, based on TCGA and The Human Protein Atlas data. The TCGA RNAseq profiles of HCC were extracted to explore the relative expression of (A) MAPK14, (B) RELA, (C) CDK2, (D) CDK4 and (E) SP1 in HCC and adjacent non-cancerous liver tissues. Immunohistochemical data was downloaded from The Human Protein Atlas. TCGA, The Cancer Genome Atlas; HCC, hepatocellular carcinoma; MAPK14, mitogen-activated protein kinase 14; RELA, RELA proto-oncogene, nuclear factor κB subunit; CDK2, cycle dependent kinase 2; CDK4, cycle dependent kinase 4; SP1, SP1 transcription factor.

downregulated in the HCC tissues when compared with adjacent non-cancerous tissues (data not shown). Notably, MAPK14, RELA, SOS1, CDK2, CDK4 and SP1 were significantly overexpressed in liver cancer tissues, compared with expression in adjacent liver tissues ($P<0.01$).

The protein expression of the six aforementioned genes was also collected, as they were more likely to be direct miR-124-3p targets. The immunohistochemical data downloaded from The Human Protein Atlas revealed that all these genes were overexpressed in HCC tissues, with the exception of SOS1, which was also positively stained in normal tissues. Therefore, MAPK14, RELA, CDK2, CDK4 and SP1 were considered direct targets of miR-124-3p in HCC. Expression profiles of the five mRNAs with their corresponding immunohistochemical results are presented in Fig. 7.

Functional and signaling pathway analyses. The 132 identified genes were classified into three GO categories using the

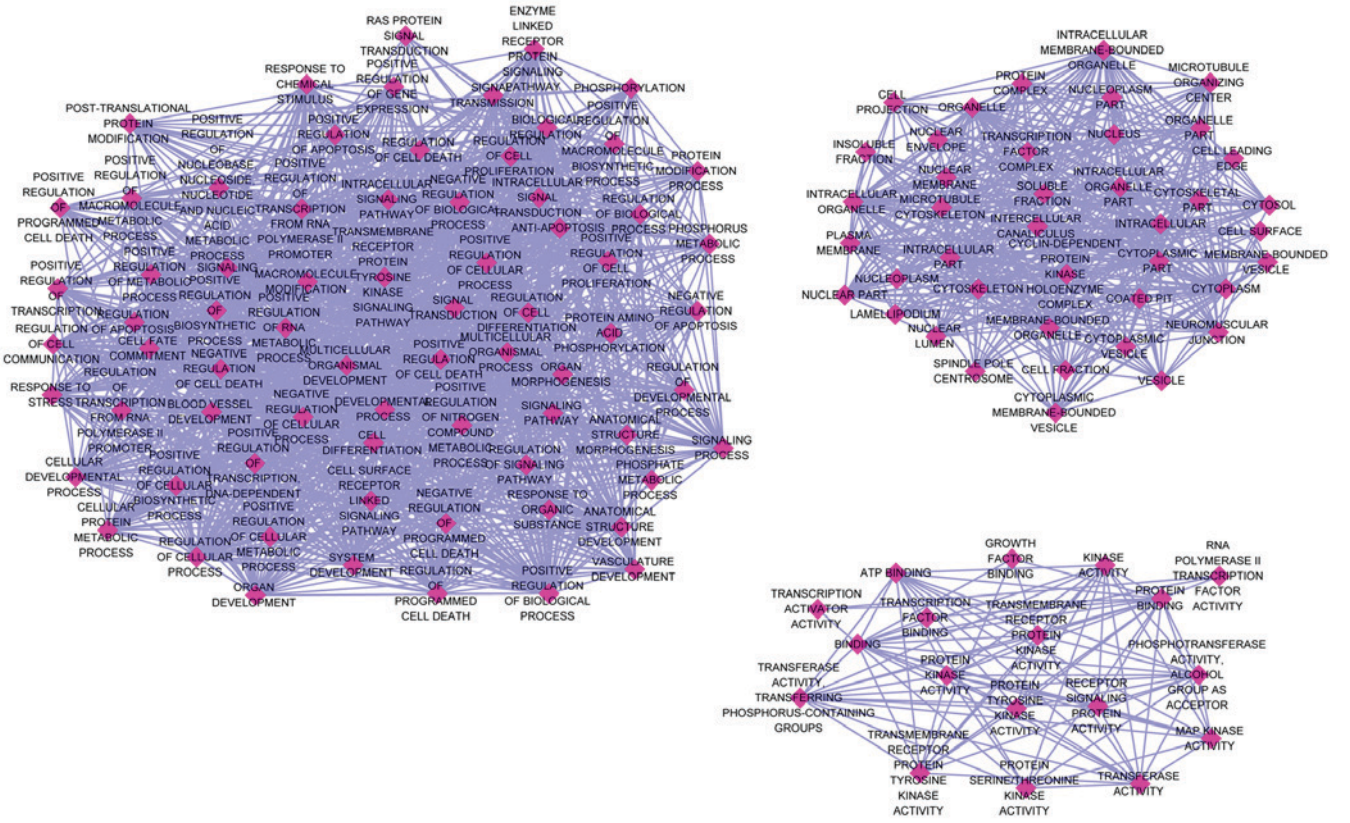

Figure 8. GO enrichment maps were drawn using the Cytoscape v3.4.0 EnrichmentMap plug-in. The rhombus represents different terms of biological processes. The associations among terms are represented by arrows. The number of nodes and edges of the three GO categories was: biological process, 72 and 1366; cellular component, 41 and 461; and molecular function, 18 and 92; respectively. GO, gene ontology.

online analysis tool DAVID. The BP genes exhibited significant enrichment in the regulation of cell proliferation (GO, 0042127; $P=1.71x10^{-10}$), positive regulation of cellular biosynthetic processes (GO, 0031328; $P=1.86x10^{-10}$) and positive regulation of biosynthetic processes (GO, 0009891; $P=2.57X10^{-10}$). Among the CC genes, the top three functional items were cell leading edge (GO, 0031252; $P=4.06x10^{-7}$), cytosol (GO, 0005829; $P=1.12x10^{-5}$) and cell projection (GO, 0042995; $P=1.18x10^{-5}$). Among the MF genes, the most clustered GO terms were protein kinase activity (GO, 0004672; $P=4.92x10^{-7}$), transcription activator activity (GO, 0016563; $P=8.83x10^{-5}$) and enzyme binding (GO, 0019899; $P=2.77x10^{-4}$). Three visualized GO maps (BP, CC and MF) were drawn by EnrichmentMap, a Cytoscape v3.4.0 plug-in. In the enrichment map, the number of nodes and edges of the three GO categories was: BP, 72 and 1366; CC, 41 and 461; MF, 18 and 92, respectively (Fig. 8). The top 10 categories for 3 GO terms are presented in Table III.

KEGG pathway enrichment analysis revealed that pancreatic cancer (hsa05212; $P=6.80x10^{-8}$), prostate cancer (hsa05215; $P=5.28x10^{-7}$), non-small cell lung cancer (hsa05223; $P=9.25x10^{-7}$), chronic myeloid leukemia (hsa05220; $P=1.16x10^{-6}$) and pathways in cancer (hsa05200; $P=3.64x10^{-6}$) had the most significant enrichment. The top 30 enriched pathways were presented using the ggplot2 (version 2.2.1) package of R/Bioconductor (version 3.4.2) Project for Statistical Computing (https://www.r-project.org/), a free software environment for statistical computing and graphics (32) (Fig. 9).

Regarding the PANTHER pathway, the following three terms were identified as the most significant: Angiogenesis (P00005; $P=1.78x10^{-7}$), epidermal growth factor receptor signaling pathway (P00018; $P=1.54x10^{-6}$), and FGF signaling pathway (P00021; $P=4.32x10^{-5}$). The top 10 categories for KEGG and the PANTHER pathway are presented in Table IV.

Discussion

The occurrence and development of HCC is a multistep process that involves the activation of tumor oncogenes and/or the inactivation of tumor suppressor genes. These factors are of vital importance for the design of effective therapeutic strategies for the treatment of HCC. Given that the prognosis of advanced HCC remains poor regardless of improvements in innovative therapeutic approaches, the development of a more effective method of diagnosis and therapy and/or a novel biomarker for early stage HCC is urgently required. Previous studies have demonstrated the crucial involvement of miRNAs in carcinogenesis (33-35). The function of miRNAs in hepatocarcinogenesis has also been assessed. The ectopic expression of several miRNAs has been detected in HCC, including miR-21, miR-542-5p, miR-29, miR-140-5p, miR-221 and miR-490-3p. Previous studies have also reported low miR-124 expression in HCC (2,10,36,37), prostate cancer (38), breast cancer (39), gastric cancer (40) and pancreatic cancer (41). In line with the results of previous studies, the present study demonstrated that miR-124-3p was downregulated in HCC and that its downregulation was significantly associated with certain clinical characteristics, including the TNM stage. Additionally, the data

Table III. GO functional annotation for most significantly associated targets of microRNA-124-3p.

GO ID	GO term	Count (%)	P-value	Benjamini	FDR	Gene symbol
Biological process						
GO:0042127	Regulation of cell proliferation	30 (1.7)	1.71×10^{-10}	2.83×10^{-7}	2.88×10^{-7}	FGFR2, FGFR1, ERBB3, ERBB2, PRRX1, CHEK1, ABI1, JAG1, SOX9, ITGB1, IL11, TGFA, ASPH, TCF3, RELA, etc..
GO:0031328	Positive regulation of cellular biosynthetic process	28 (1.6)	1.86×10^{-10}	1.54×10^{-7}	3.13×10^{-7}	PPARA, SOX9, TLR7, IL11, ZNF148, SQSTM1, YAP1, TCF4, TCF3, AKT2, EGR1, SREBF1, RELA, GRIN1, SMAD5, etc.
GO:0009891	Positive regulation of biosynthetic process	28 (1.6)	2.57×10^{-10}	1.42×10^{-7}	4.32×10^{-7}	PPARA, SOX9, TLR7, IL11, ZNF148, SQSTM1, YAP1, TCF4, TCF3, AKT2, EGR1, SREBF1, RELA, GRIN1, SMAD5, etc.
GO:0045944	Positive regulation of transcription from RNA polymerase II promoter	21 (1.2)	2.78×10^{-10}	1.15×10^{-7}	4.68×10^{-7}	SREBF1, EGR1, PPARA, RELA, SMAD5, GRIN1, SMAD4, SOX9, AHR, IL11, HDAC4, SP1, ZNF148, SQSTM1, ETS1, etc.
GO:0010557	Positive regulation of macromolecule biosynthetic process	27 (1.5)	3.57×10^{-10}	1.18×10^{-7}	6.00×10^{-7}	PPARA, SOX9, TLR7, IL11, ZNF148, SQSTM1, YAP1, TCF4, TCF3, AKT2, EGR1, SREBF1, RELA, GRIN1, SMAD5, etc.
GO:0006468	Protein amino acid phosphorylation	27 (1.5)	5.45×10^{-10}	1.50×10^{-7}	9.16×10^{-7}	FGFR2, FGFR1, ERBB3, ERBB2, ABI1, AURKA, CHEK1, TGFA, PIK3CA, AKT2, ROCK1, CDK6, MAPK10, CDK4, CDK2, etc.
GO:0042981	Regulation of apoptosis	29 (1.7)	1.35×10^{-9}	3.20×10^{-7}	2.28×10^{-6}	ING3, HTATIP2, ERBB3, ERBB2, BCL2L2, SOX9, PEA15, CD44, SQSTM1, SOS1, PIK3CA, ARHGDIA, RAB27A, ROCK1, RELA, etc.
GO:0043067	Regulation of programmed cell death	29 (1.7)	1.69×10^{-9}	3.49×10^{-7}	2.84×10^{-6}	ING3, HTATIP2, ERBB3, ERBB2, BCL2L2, SOX9, PEA15, CD44, SQSTM1, SOS1, PIK3CA, ARHGDIA, RAB27A, ROCK1, RELA, etc.
GO:0010941	Regulation of cell death	29 (1.7)	1.84×10^{-9}	3.37×10^{-7}	3.08×10^{-6}	ING3, HTATIP2, ERBB3, ERBB2, BCL2L2, SOX9, PEA15, CD44, SQSTM1, SOS1, PIK3CA, ARHGDIA, RAB27A, ROCK1, RELA, etc.
GO:0045941	Positive regulation of transcription	24 (1.4)	2.67×10^{-9}	4.42×10^{-7}	4.49×10^{-6}	SREBF1, EGR1, PPARA, RELA, SMAD5, GRIN1, SMAD4, SOX9, AHR, CDK2, IL11, HDAC4, MAPK1, SP1, ZNF148, etc.
Cellular component						
GO:0031252	Cell leading edge	11 (0.6)	4.06×10^{-7}	9.92×10^{-5}	5.26×10^{-4}	SPRY1, TLN2, GSN, WASF2, ARHGAP1, PIK3CA, ABI1, CDK6, ITGB1, IQGAP1, AKT2
GO:0005829	Cytosol	29 (1.7)	1.12×10^{-5}	0.00136	0.01446	VIM, BCL2L2, ABI1, ANXA7, SPRY2, SPRY1, GSN, SQSTM1, SOS1, PIK3CA, ARHGDIA, AKT2, ROCK1, RELA, SMAD5, etc.
GO:0042995	Cell projection	20 (1.1)	1.18×10^{-5}	9.61×10^{-4}	0.01530	TLN2, ERBB2, VIM, GRIN1, WASF2, CDK6, ABI1, ITGB1, IQGAP1, MAPK1, EPHA7, SPRY1, LRP1, PSEN1, GSN, etc.
GO:0005667	Transcription factor complex	11 (0.6)	1.78×10^{-5}	0.00109	0.02304	GSC, E2F5, RELA, SMAD5, SMAD4, YAP1, TCF4, CDK4, TCF3, KLF4, CDK2
GO:0000267	Cell fraction	23 (1.3)	2.00×10^{-4}	0.00970	0.25820	FGFR1, GYPA, GRIN1, SPHK1, ABI1, CAPN2, ITGB1, BCL2L11, PTPN12, SOD2, ANXA7, MAPK1, LRP1, PSEN1, ARAF, etc.
GO:0009986	Cell surface	12 (0.7)	2.74×10^{-4}	0.01108	0.35385	FGFR2, LRP1, PSEN1, PRLR, CD44, SULF1, PVRL2, TGFA, SORT1, IL7R, ITGB1, DPP4
GO:0005654	Nucleoplasm	20 (1.1)	2.79×10^{-4}	0.00967	0.35999	ING3, GSC, E2F5, RELA, SMAD5, SMAD4, CHEK1, CDK4, SART3, CDK2, CDC25B, HDAC4, MAPK1, SQSTM1, etc.
GO:0031981	Nuclear lumen	27 (1.5)	3.55×10^{-4}	0.01078	0.45888	ING3, E2F5, CHEK1, SOX9, SART3, IQGAP1, ZNF148, SQSTM1, YAP1, TCF4, MYB, TCF3, ZBTB20, GSC, RELA, etc.
GO:0030027	Lamellipodium	6 (0.3)	3.94×10^{-4}	0.01063	0.50892	SPRY1, GSN, WASF2, PIK3CA, ABI1, AKT2
GO:0005856	Cytoskeleton	26 (1.5)	4.10×10^{-4}	0.00996	0.52974	TLN2, VIM, WASF2, ABI1, AURKA, ABCA2, CHEK1, SEC62, IQGAP1, SPRY2, PEA15, GSN, SOS1, ARHGDIA, KIF14, etc.

Table III. Continued.

GO ID	GO term	Count (%)	P-value	Benjamini	FDR	Gene symbol
Molecular function						
GO:0004672	Protein kinase activity	21 (1.2)	4.92×10^{-7}	1.73×10^{-4}	6.73×10^{-4}	FGFR2, FGFR1, ROCK1, ERBB3, ERBB2, CDK6, CHEK1, AURKA, MAPK10, CDK4, CDK2, EPHA3, MAPK1, EPHA7, CRKL, etc.
GO:0016563	Transcription activator activity	14 (0.8)	8.83×10^{-5}	0.01542	0.12078	EGR1, PPARA, HTATIP2, SMAD5, SMAD4, PRRX1, SOX9, HDAC4, SP1, ZNF148, YAP1, MYB, TCF3, KLF4
GO:0019899	Enzyme binding	15 (0.9)	2.77×10^{-4}	0.03193	0.37791	FMNL2, ROCK1, ERBB2, RELA, VIM, CHEK1, AURKA, IQGAP1, HDAC4, SPAG9, MAPK1, LRP1, SP1, SQSTM1, SORT1
GO:0004714	Transmembrane receptor protein tyrosine kinase activity	6 (0.3)	3.51×10^{-4}	0.03042	0.47936	FGFR2, FGFR1, EPHA7, ERBB3, ERBB2, EPHA3
GO:0004674	Protein serine/threonine kinase activity	13 (0.7)	5.34×10^{-4}	0.03689	0.72816	ROCK1, AURKA, CHEK1, CDK6, MAPK10, CDK4, CDK2, MAPK1, MAPK14, ARAF, HIPK2, ERN1, AKT2
GO:0005524	ATP binding	26 (1.5)	0.00148	0.08344	2.01226	FGFR2, FGFR1, ERBB3, ERBB2, ABCA2, AURKA, CHEK1, PIK3CA, AKT2, KIF14, ROCK1, G3BP1, SPHK1, CDK6, etc.
GO:0003702	RNA polymerase II transcription factor activity	9 (0.5)	0.00172	0.08284	2.32651	SREBF1, PPARA, HTATIP2, SP1, ETS1, ZNF148, RELA, SOX9, KLF4
GO:0010843	Promoter binding	5 (0.3)	0.00177	0.07487	2.39182	SREBF1, HDAC4, SP1, SMAD4, TCF3
GO:0032559	Adenyl ribonucleotide binding	26 (1.5)	0.00179	0.06771	2.42412	FGFR2, FGFR1, ERBB3, ERBB2, ABCA2, AURKA, CHEK1, PIK3CA, AKT2, KIF14, ROCK1, G3BP1, SPHK1, CDK6, etc.
GO:0019838	Growth factor binding	6 (0.3)	0.00267	0.08983	3.59394	ERBB3, CTGF, ERBB2, SORT1, IL7R, IGFBP3

GO, gene ontology.

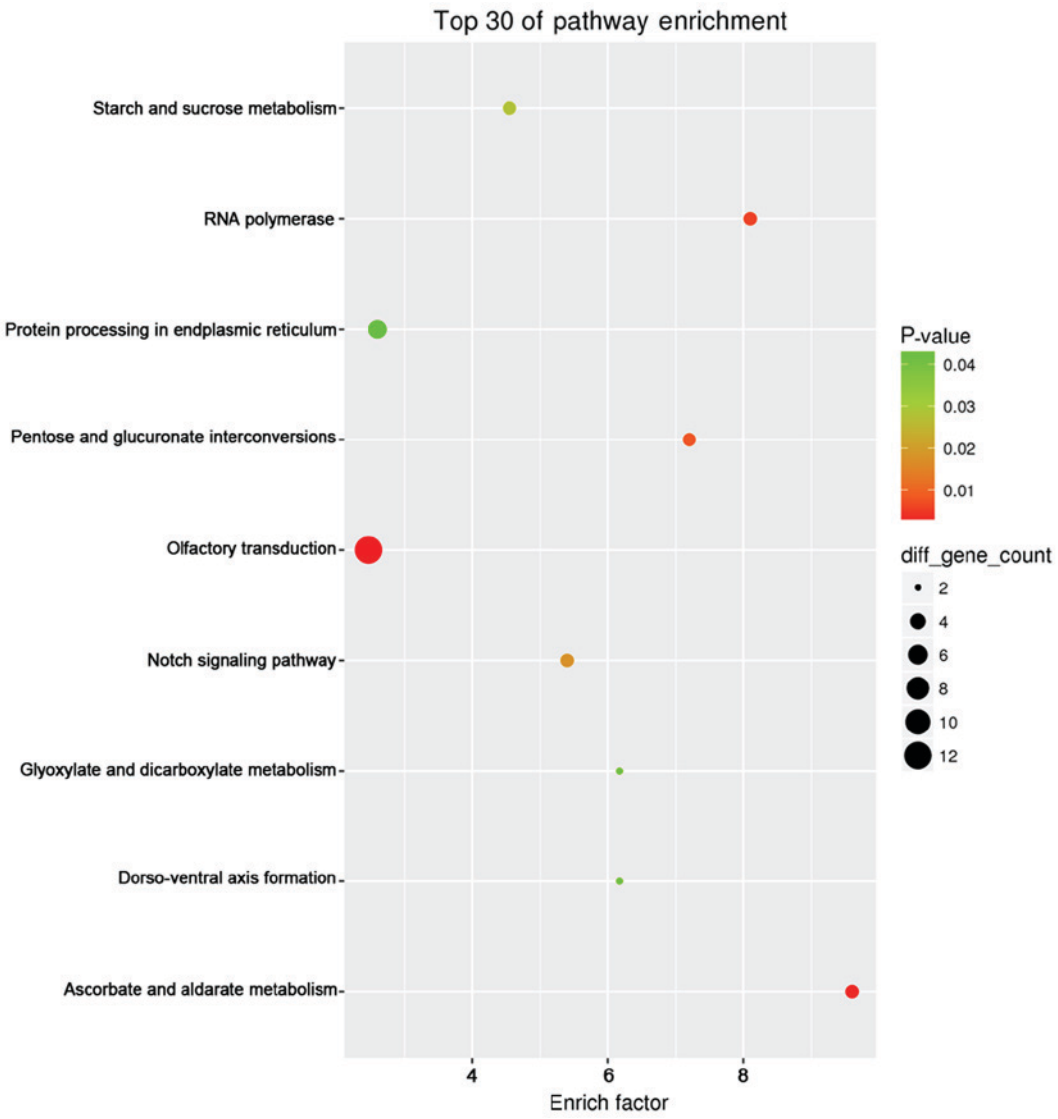

Figure 9. KEGG pathway analysis of microRNA 124-3p predicted target genes in hepatocellular carcinoma. Enrichment analysis was performed to identify pathways enriched in olfactory transduction using the ggplot2 (version 2.2.1) package of R/Bioconductor (version 3.4.2) Project for Statistical Computing (https://www.r-project.org/). KEGG, Kyoto Encyclopedia of Genes and Genomes.

indicated that miR-124-3p expression is positively associated with RFS in patients with HCC (P=0.012). Meta-analysis of GEO data only, and meta-analysis of GEO data plus in-house PCR revealed no significant difference of miR-124-3p between HCC and non-cancerous liver groups. Certain chips contained fewer HCC samples than non-cancerous samples, while other chips contained more HCC samples than non-cancerous samples. Additionally, technology may be another cause of this difference. For example, amongst the data included here, certain parts were detected using gene chip technology, while a number were detected by PCR. Conversely, seven microarrays come from different platforms, which is another reason to cause the difference. TCGA was used in order to validate the downregulation of miR-124-3p, but this was unsuccessful due to the lack of available data.

miRNAs are a class of short endogenous non-coding RNAs that inhibit gene expression by either degrading mRNA or repressing mRNA translation. Theoretically, there are hundreds of potential targets for a single miRNA. Previous studies have demonstrated that miRNAs modulate a wide variety of targets, indicating that a single miRNA may regulate cancer progression in multiple steps by targeting numerous genes. Zheng *et al* (37) reported that miR-124 inhibits epithelial-mesenchymal transition by inhibiting the mRNA and protein expression of ROCK2 and EZH2 in HCC. Lang and Ling (10) demonstrated that miR-124 inhibits cell proliferation by targeting PIK3CA in HCC. The literature search of the present study revealed that miR-124-3p acts via the regulation of CTGF, ITGB1, RhoG and ROCK1 expression. Recently, with the progression of high-throughput sequencing and bioinformatics, circular RNAs (circRNAs) have received increasing attention (42,43). Increasing evidence indicates that circRNAs may serve a major role in various types of cancer (44-46), including HCC. Shang *et al* (47) identified hsa_circ_0005075 as a potential HCC biomarker involved in HCC development. Qin *et al* (48) and Xu *et al* (49) also demonstrated that circRNAs may serve as potential novel biomarkers in HCC. Notably, Zheng *et al* (50) performed RNA immunoprecipitation and luciferase screening, demonstrating that circHIPK3 may function as a sponge for miRNAs, including miR-12, as circHIPK3 is directly adsorbed

Table IV. KEGG and PANTHER functional annotation for most significantly associated targets of miR-124-3p.

Database ID	Database term	Count (%)	P-value	Benjamini	FDR	Gene symbol
KEGG						
hsa05212	Pancreatic cancer	11 (0.6)	6.80×10^{-8}	6.39×10^{-6}	7.46×10^{-5}	MAPK1, RELA, ERBB2, ARAF, SMAD4, TGFA, PIK3CA, CDK6, MAPK10, CDK4, AKT2
hsa05215	Prostate cancer	11 (0.6)	5.28×10^{-7}	2.48×10^{-5}	5.79×10^{-4}	FGFR2, FGFR1, MAPK1, RELA, ERBB2, SOS1, ARAF, TGFA, PIK3CA, CDK2, AKT2
hsa05223	Non-small cell lung cancer	9 (0.5)	9.25×10^{-7}	2.90×10^{-5}	0.00101	MAPK1, ERBB2, SOS1, ARAF, TGFA, PIK3CA, CDK6, CDK4, AKT2
hsa05220	Chronic myeloid leukemia	10 (0.6)	1.16×10^{-6}	2.74×10^{-5}	0.00128	MAPK1, CRKL, RELA, SOS1, ARAF, SMAD4, PIK3CA, CDK6, CDK4, AKT2
hsa05200	Pathways in cancer	18 (1.0)	3.64×10^{-6}	6.84×10^{-5}	0.00399	FGFR2, FGFR1, ERBB2, RELA, SMAD4, CDK6, MAPK10, CDK4, ITGB1, CDK2, MAPK1, CRKL, ETS1, SOS1, ARAF, TGFA, PIK3CA, AKT2
hsa04012	ErbB signaling pathway	10 (0.6)	4.13×10^{-6}	6.47×10^{-5}	0.00453	MAPK1, CRKL, ERBB3, ERBB2, SOS1, ARAF, TGFA, PIK3CA, MAPK10, AKT2
hsa04722	Neurotrophin signaling pathway	11 (0.6)	1.12×10^{-5}	1.51×10^{-4}	0.01230	MAPK1, CRKL, PSEN1, RELA, MAPK14, SOS1, SORT1, PIK3CA, MAPK10, ARHGDIA, AKT2
hsa05214	Glioma	8 (0.5)	3.27×10^{-5}	3.84×10^{-4}	0.03585	MAPK1, SOS1, ARAF, TGFA, PIK3CA, CDK6, CDK4, AKT2
hsa05211	Renal cell carcinoma	8 (0.5)	6.52×10^{-5}	6.81×10^{-4}	0.07153	MAPK1, CRKL, ETS1, SOS1, ARAF, TGFA, PIK3CA, AKT2
hsa04520	Adherens junction	8 (0.5)	1.21×10^{-4}	0.00113	0.13211	FGFR1, MAPK1, TJP1, ERBB2, WASF2, PVRL2, SMAD4, IQGAP1
PANTHER						
P00005	Angiogenesis	17 (1.0)	1.78×10^{-7}	8.17×10^{-6}	1.68×10^{-4}	FGFR2, FGFR1, SPHK1, JAG1, MAPK10, EPHA3, MAPK1, EPHA7, CRKL, ETS1, MAPK14, SOS1, ARAF, ARHGAP1, etc.
P00018	EGF receptor signaling pathway	13 (0.7)	1.54×10^{-6}	3.55×10^{-5}	0.00146	MAPK1, SPRY2, DAB2IP, SPRY1, ERBB3, MAPK14, ERBB2, SOS1, ARAF, PIK3CA, TGFA, MAPK10, AKT2
P00021	FGF signaling pathway	11 (0.6)	4.32×10^{-5}	6.61×10^{-4}	0.04078	FGFR2, SPRY2, FGFR1, MAPK1, SPRY1, MAPK14, SOS1, ARAF, PIK3CA, MAPK10, AKT2
P00056	VEGF signaling pathway	8 (0.5)	2.25×10^{-4}	0.00259	0.21257	MAPK1, ETS1, MAPK14, ARAF, ARHGAP1, SPHK1, PIK3CA, AKT2
P04393	Ras Pathway	8 (0.5)	5.48×10^{-4}	0.00503	0.51707	MAPK1, ETS1, MAPK14, SOS1, ARAF, PIK3CA, MAPK10, AKT2
P00010	B cell activation	6 (0.3)	0.01190	0.08766	10.69454	MAPK1, MAPK14, SOS1, ARAF, PIK3CA, MAPK10
P00006	Apoptosis signaling pathway	7 (0.4)	0.01767	0.11053	15.50490	MAPK1, TNFRSF10B, RELA, PIK3CA, BCL2L2, MAPK10, AKT2
P04398	p53 pathway feedback loops 2	5 (0.3)	0.01786	0.09846	15.66488	MAPK14, PIK3CA, CCNG2, CDK2, AKT2
P00054	Toll receptor signaling pathway	5 (0.3)	0.01987	0.09748	17.27652	MAPK1, RELA, MAPK14, MAPK10, TLR7
P00034	Integrin signaling pathway	9 (0.5)	0.02426	0.10682	20.71556	MAPK1, CRKL, MAPK14, SOS1, ARAF, PIK3CA, MAPK10, ITGB1, PTPN12
P00047	PDGF signaling pathway	8 (0.5)	0.02650	0.10625	22.42248	MAPK1, ETS1, SOS1, ARAF, ARHGAP1, PIK3CA, MAPK10, AKT2
P00053	T cell activation	6 (0.3)	0.04509	0.16213	35.34827	MAPK1, SOS1, ARAF, PIK3CA, MAPK10, AKT2
P00059	p53 pathway	6 (0.3)	0.04510	0.16213	35.34827	TNFRSF10B, PIK3CA, IGFBP3, CCNG2, CDK2, AKT2

KEGG, Kyoto encyclopedia of genes and genomes; PANTHER, protein annotation through evolutionary relationship.

to miR-124 and suppresses its activation. In the present study, the target genes of miR-124-3p were explored by assessing the overlapping genes retrieved from GEO profiles, prediction software and NLP. A total of 132 potential target mRNAs of miR-124-3p in HCC were identified. Based on the prospective roles of circRNAs in human cancer, future studies should aim to further investigate the association between circRNA and miR-124-3p in HCC.

As the diagnosis of HCC at early stages is difficult, when patients were diagnosed with HCC, it is generally too late to remove the tumor with surgical excision. Various novel therapies for advanced HCC are being actively pursued, including molecular targeted therapy, systemic chemotherapy, immunotherapy and arginine deprivation therapy (51). These treatment therapies are all involved in the molecular pathways of HCC development. Furthermore, the majority of the molecular targeted drugs currently being investigated are multi-targeted drugs. Therefore, it is crucial to elucidate the molecular pathogenesis of HCC. Following the prediction of potential target genes, functional and signaling pathway analyses were conducted. Additionally, enriched GO term, KEGG pathway and PANTHER pathway analyses of miR-124-3p target genes were performed. The results revealed that the predicted target genes of miR-124-3p involved 396 GO terms. The top-ranking terms all exhibited a large number of gene clusters, particularly in BP terms. KEGG pathway enrichment analysis demonstrated that the predicted target genes of miR-124-3p were concentrated in 41 signaling pathways, and the top ten signaling pathways were involved in the occurrence and development of several types of cancer. PANTHER pathway analysis indicated that the predicted target genes of miR-124-3p were concentrated in 14 terms, which were all involved in various molecular signaling pathways. Therefore, taken together with the results of previous studies, these observations suggested that miR-124-3p may target multiple genes and may function spatiotemporally or in combination with several diverse processes. For example, among the 14 terms of the PANTHER pathway, 'Angiogenesis', 'EGF receptor signaling pathway', 'FGF signaling pathway', 'VEGF signaling pathway' and 'PDGF signaling pathway' are all involved in angiogenesis. However, other target genes involved in 'B cell activation', 'Toll receptor signaling pathway' and 'T cell activation' indicated that immunological mechanisms may be the other factor that affected the genesis and the development of HCC. In addition, 'Ras pathway', 'Apoptosis signaling pathway' and 'P53 pathway' have also been predicted. Further research on the mechanisms of above pathway may be beneficial in the development of novel therapeutic agents against HCC.

In conclusion, it was confirmed that miR-124-3p was downregulated in HCC. Assessing the overlaps in GEO data, miR-124-3p predicted target genes and NLP, 132 reliable potential target genes of miR-124-3p were identified that may serve key functions in HCC. The pathway analysis results suggested that the functional characterization of the identified miR-124-3p targets will offer novel insight into the underlying molecular mechanisms that occur in HCC. Given the complexity of molecular pathway involvement, the mechanism of hepatocarcinogenesis requires further study with powerful analysis tools, as well as through the study of *in vitro* and *in vivo* models. The identified miR-124-3p target genes have the potential to be employed as innovative prognosticators and/or therapeutic targets for HCC.

Competing interests

The authors declare that they have no competing interests.

References

1. Huang DH, Wang GY, Zhang JW, Li Y, Zeng XC and Jiang N: MiR-501-5p regulates CYLD expression and promotes cell proliferation in human hepatocellular carcinoma. Jpn J Clin Oncol 45: 738-744, 2015.
2. Lu Y, Yue X, Cui Y, Zhang J and Wang K: MicroRNA-124 suppresses growth of human hepatocellular carcinoma by targeting STAT3. Biochem Biophys Res Commun 441: 873-879, 2013.
3. Otsuka M, Kishikawa T, Yoshikawa T, Yamagami M, Ohno M, Takata A, Shibata C, Ishibashi R and Koike K: MicroRNAs and liver disease. J Hum Genet 62: 75-80, 2017.
4. Huang Y, Shen XJ, Zou Q, Wang SP, Tang SM and Zhang GZ: Biological functions of microRNAs: A review. J Physiol Biochem 67: 129-139, 2011.
5. Torre LA, Bray F, Siegel RL, Ferlay J, Lortet-Tieulent J and Jemal A: Global cancer statistics, 2012. CA Cancer J Clin 65: 87-108, 2015.
6. Bosch FX, Ribes J, Diaz M and Cleries R: Primary liver cancer: Worldwide incidence and trends. Gastroenterology 127 (5 Suppl 1): S5-S16, 2004.
7. Sherman M: Hepatocellular carcinoma: Epidemiology, surveillance, and diagnosis. Semin Liver Dis 30: 3-16, 2010.
8. Shangguan H, Tan SY and Zhang JR: Bioinformatics analysis of gene expression profiles in hepatocellular carcinoma. Eur Rev Med Pharmacol Sci 19: 2054-2061, 2015.
9. Huang S and He X: The role of microRNAs in liver cancer progression. Br J Cancer 104: 235-240, 2011.
10. Lang Q and Ling C: MiR-124 suppresses cell proliferation in hepatocellular carcinoma by targeting PIK3CA. Biochem Biophys Res Commun 426: 247-252, 2012.
11. Furuta M, Kozaki KI, Tanaka S, Arii S, Imoto I and Inazawa J: miR-124 and miR-203 are epigenetically silenced tumor-suppressive microRNAs in hepatocellular carcinoma. Carcinogenesis 31: 766-776, 2010.
12. World Health Organization (WHO): WHO Handbook for Reporting Results of Cancer Treatment. WHO, Geneva, 1979.
13. Rong M, He R, Dang Y and Chen G: Expression and clinicopathological significance of miR-146a in hepatocellular carcinoma tissues. Ups J Med Sci 119: 19-24, 2014.
14. Rong M, Chen G and Dang Y: Increased miR-221 expression in hepatocellular carcinoma tissues and its role in enhancing cell growth and inhibiting apoptosis in vitro. BMC Cancer 13: 21, 2013.
15. Chen G, Umelo IA, Lv S, Teugels E, Fostier K, Kronenberger P, Dewaele A, Sadones J, Geers C and De Grève J: miR-146a inhibits cell growth, cell migration and induces apoptosis in non-small cell lung cancer cells. PLoS One 8: e60317, 2013.
16. Liu Y, Ren F, Luo Y, Rong M, Chen G and Dang Y: Down-regulation of miR-193a-3p dictates deterioration of HCC: A clinical real-time qRT-PCR study. Med Sci Monit 21: 2352-2360, 2015.
17. Livak KJ and Schmittgen TD: Analysis of relative gene expression data using real-time quantitative PCR and the 2(-Delta Delta C(T)) method. Methods 25: 402-408, 2001.
18. Egger M, Smith GD and Altman DG (eds): Systematic Reviews in Health Care. Meta-analysis in Context. 2nd edition. BMJ Publishing Group, London, 2001.
19. Murakami Y, Kubo S, Tamori A, Itami S, Kawamura E, Iwaisako K, Ikeda K, Kawada N, Ochiya T and Taguchi YH: Comprehensive analysis of transcriptome and metabolome analysis in Intrahepatic Cholangiocarcinoma and Hepatocellular Carcinoma. Sci Rep 5: 16294, 2015.
20. Diaz G, Melis M, Tice A, Kleiner DE, Mishra L, Zamboni F and Farci P: Identification of microRNAs specifically expressed in hepatitis C virus-associated hepatocellular carcinoma. Int J Cancer 133: 816-824, 2013.
21. Sato F, Hatano E, Kitamura K, Myomoto A, Fujiwara T, Takizawa S, Tsuchiya S, Tsujimoto G, Uemoto S and Shimizu K: MicroRNA profile predicts recurrence after resection in patients with hepatocellular carcinoma within the Milan criteria. PLoS One 6: e16435, 2011.

22. He XX, Chang Y, Meng FY, Wang MY, Xie QH, Tang F, Li PY, Song YH and Lin JS: MicroRNA-375 targets AEG-1 in hepatocellular carcinoma and suppresses liver cancer cell growth in vitro and in vivo. Oncogene 31: 3357-3369, 2012.
23. Su H, Yang JR, Xu T, Huang J, Xu L, Yuan Y and Zhuang SM: MicroRNA-101, down-regulated in hepatocellular carcinoma, promotes apoptosis and suppresses tumorigenicity. Cancer Res 69: 1135-1142, 2009.
24. Wang PR, Xu M, Toffanin S, Li Y, Llovet JM and Russell DW: Induction of hepatocellular carcinoma by in vivo gene targeting. Proc Natl Acad Sci USA 109: 11264-11269, 2012.
25. Wang X and Wang X: Systematic identification of microRNA functions by combining target prediction and expression profiling. Nucleic Acids Res 34: 1646-1652, 2006.
26. Dweep H and Gretz N: miRWalk2.0: A comprehensive atlas of microRNA-target interactions. Nat Methods 12: 697, 2015.
27. Chang EK, Yu CY, Clarke R, Hackbarth A, Sanders T, Esrailian E, Hommes DW and Runyon BA: Defining a patient population with cirrhosis: An automated algorithm with natural language processing. J Clin Gastroenterol 50: 889-894, 2016.
28. Alsawas M, Alahdab F, Asi N, Li DC, Wang Z and Murad MH: Natural language processing: Use in EBM and a guide for appraisal. Evid Based Med 21: 136-138, 2016.
29. Zhang X, Tang W, Chen G, Ren F, Liang H, Dang Y and Rong M: An encapsulation of gene signatures for hepatocellular carcinoma, microRNA-132 predicted target genes and the corresponding overlaps. PLoS One 11: e0159498, 2016.
30. Huang WT, Wang HL, Yang H, Ren FH, Luo YH, Huang CQ, Liang YY, Liang HW, Chen G and Dang YW: Lower expressed miR-198 and its potential targets in hepatocellular carcinoma: A clinicopathological and in silico study. Onco Targets Ther 9: 5163-5180, 2016.
31. Liese J, Peveling-Oberhag J, Doering C, Schnitzbauer AA, Herrmann E, Zangos S, Hansmann ML, Moench C, Welker MW, Zeuzem S, *et al*: A possible role of microRNAs as predictive markers for the recurrence of hepatocellular carcinoma after liver transplantation. Transpl Int 29: 369-380, 2016.
32. Ito K and Murphy D: Application of ggplot2 to Pharmacometric Graphics. CPT Pharmacometrics Syst Pharmacol 2: e79, 2013.
33. Xu C, Zeng Q, Xu W, Jiao L, Chen Y, Zhang Z, Wu C, Jin T, Pan A, Wei R, *et al*: miRNA-100 inhibits human bladder urothelial carcinogenesis by directly targeting mTOR. Mol Cancer Ther 12: 207-219, 2013.
34. Ma Y, Han W, Yang L, He L and Wang H: The regulation of miRNAs in inflammation-related carcinogenesis. Curr Pharm Des 21: 3023-3031, 2015.
35. Wan X, Ding X, Chen S, Song H, Jiang H, Fang Y, Li P and Guo J: The functional sites of miRNAs and lncRNAs in gastric carcinogenesis. Tumour Biol 36: 521-532, 2015.
36. Xu L, Dai W, Li J, He L1, Wang F, Xia Y, Chen K, Li S, Liu T, Lu J, *et al*: Methylation-regulated miR-124-1 suppresses tumorigenesis in hepatocellular carcinoma by targeting CASC3. Oncotarget 7: 26027-26041, 2016.
37. Zheng F, Liao YJ, Cai MY, Liu YH, Liu TH, Chen SP, Bian XW, Guan XY, Lin MC, Zeng YX, *et al*: The putative tumour suppressor microRNA-124 modulates hepatocellular carcinoma cell aggressiveness by repressing ROCK2 and EZH2. Gut 61: 278-289, 2012.
38. Shi XB, Xue L, Ma AH, Tepper CG, Gandour-Edwards R, Kung HJ and deVere White RW: Tumor suppressive miR-124 targets androgen receptor and inhibits proliferation of prostate cancer cells. Oncogene 32: 4130-4138, 2013.
39. Lv XB, Jiao Y, Qing Y, Hu H, Cui X, Lin T, Song E and Yu F: miR-124 suppresses multiple steps of breast cancer metastasis by targeting a cohort of pro-metastatic genes in vitro. Chin J Cancer 30: 821-830, 2011.
40. Li H, Xie S, Liu M, Chen Z, Liu X, Wang L, Li D and Zhou Y: The clinical significance of downregulation of mir-124-3p, mir-146a-5p, mir-155-5p and mir-335-5p in gastric cancer tumorigenesis. Int J Oncol 45: 197-208, 2014.
41. Wang P, Chen L, Zhang J, Chen H, Fan J, Wang K, Luo J, Chen Z, Meng Z and Liu L: Methylation-mediated silencing of the miR-124 genes facilitates pancreatic cancer progression and metastasis by targeting Rac1. Oncogene 33: 514-524, 2014.
42. Zhao W, Cheng Y, Zhang C, You Q, Shen X, Guo W and Jiao Y: Genome-wide identification and characterization of circular RNAs by high throughput sequencing in soybean. Sci Rep 7: 5636, 2017.
43. Becker HF, Heliou A, Djaout K, Lestini R, Regnier M and Myllykallio H: High-throughput sequencing reveals circular substrates for an archaeal RNA ligase. RNA Biology 14: 1075-1085, 2017.
44. Nair AA, Niu N, Tang X, Thompson KJ, Wang L, Kocher JP, Subramanian S and Kalari KR: Circular RNAs and their associations with breast cancer subtypes. Oncotarget 7: 80967-80979, 2016.
45. Wang X, Zhang Y, Huang L, Zhang J, Pan F, Li B, Yan Y, Jia B, Liu H, Li S and Zheng W: Decreased expression of hsa_circ_001988 in colorectal cancer and its clinical significances. Int J Clin Exp Pathol 8: 16020-16025, 2015.
46. Li P, Chen S, Chen H, Mo X, Li T, Shao Y, Xiao B and Guo J: Using circular RNA as a novel type of biomarker in the screening of gastric cancer. Clin Chim Acta 444: 132-136, 2015.
47. Shang X, Li G, Liu H, Li T, Liu J, Zhao Q and Wang C: Comprehensive circular RNA profiling reveals that hsa_circ_0005075, a new circular RNA biomarker, is involved in hepatocellular crcinoma development. Medicine (Baltimore) 95: e3811, 2016.
48. Qin M, Liu G, Huo X, Tao X, Sun X, Ge Z, Yang J, Fan J, Liu L and Qin W: Hsa_circ_0001649: A circular RNA and potential novel biomarker for hepatocellular carcinoma. Cancer Biomark 16: 161-169, 2016.
49. Xu L, Zhang M, Zheng X, Yi P, Lan C and Xu M: The circular RNA ciRS-7 (Cdr1as) acts as a risk factor of hepatic microvascular invasion in hepatocellular carcinoma. J Cancer Res Clin Oncol 143: 17-27, 2017.
50. Zheng Q, Bao C, Guo W, Li S, Chen J, Chen B, Luo Y, Lyu D, Li Y, Shi G, *et al*: Circular RNA profiling reveals an abundant circHIPK3 that regulates cell growth by sponging multiple miRNAs. Nat Commun 7: 11215, 2016.
51. Gong XL and Qin SK: Progress in systemic therapy of advanced hepatocellular carcinoma. World J Gastroenterol 22: 6582-6594, 2016.

This work is licensed under a Creative Commons Attribution-NonCommercial-NoDerivatives 4.0 International (CC BY-NC-ND 4.0) License.